Deep water variability on the southern Agulhas Plateau: Interhemispheric links over the past 170 ka

Elizabeth G. Molyneux,[1] Ian R. Hall,[1] Rainer Zahn,[2] and Paula Diz[1]

Received 14 December 2006; revised 8 June 2007; accepted 29 June 2007; published 13 November 2007.

[1] Sortable silt mean grain sizes together with oxygen and carbon isotopic data produced on the benthic foraminiferal species *Fontbotia wuellerstorfi* are used to construct high-resolution records of near-bottom flow vigour and deep water ventilation at a core site MD02-2589 located at 2660 m water depth on the southern Agulhas Plateau. The results suggest that during glacial periods (marine oxygen isotope stages 2 and 6, MIS 2 and MIS 6, respectively), there was a persistent contribution of a well-ventilated water mass within the Atlantic to Indian oceanic gateway with a $\delta^{13}C$ signature similar to present-day Northern Component Water (NCW), e.g., North Atlantic Deep Water (NADW). The records of chemical ventilation and near-bottom flow vigor reflect changes in the advection of northern source waters and meridional variability in the location of the Antarctic Circumpolar Current and its associated fronts. We suggest that during Termination II (TII), changes in chemical ventilation are largely decoupled from near-bottom physical flow speeds. A mid-TII climate optimum is associated with a low-flow speed plateau concurrent with a period of increased ventilation shown in the benthic $\delta^{13}C$ of other Southern Ocean records but not in our benthic $\delta^{13}C$ of MD02-2589. The climate optimum is followed by a period of southern cooling around 128 ka coincident with a stronger influence of NCW to interglacial levels at around 124 ka. All proxy records show a near synchronous and rapid shift during the transition from MIS 5a-4 (73 ka). This large event is attributed to a rapid decrease in NADW influence and replacement over the Agulhas Plateau by southern source waters.

Citation: Molyneux, E. G., I. R. Hall, R. Zahn, and P. Diz (2007), Deep water variability on the southern Agulhas Plateau: Interhemispheric links over the past 170 ka, *Paleoceanography*, *22*, PA4209, doi:10.1029/2006PA001407.

1. Introduction

[2] A key element of the global ocean thermohaline circulation (THC) is the oceanic connection between the Indian and South Atlantic Oceans off South Africa [*de Ruijter et al.*, 1999; *Sloyan and Rintoul*, 2001] (Figure 1). Variable amounts of warm, salt-enriched South Indian Ocean waters enter the South Atlantic, the so-called ''warm water return route'' (the ''cold water return route'' being through the Drake Passage), and provide a source for heat and salt to the Atlantic thermocline that ultimately preconditions the Atlantic meridional overturning circulation for convection in the north, the formation of North Atlantic Deep Water (NADW) [*Richardson et al.*, 2003]. This westward surface return flow is compensated at depth by an eastward setting deep flow into the Indian Ocean that consists of NADW exiting the South Atlantic and the Antarctic Circumpolar Current (ACC) [*Gordon*, 1996; *Lutjeharms*, 1996].

[3] Numerous studies from the North Atlantic suggest that NADW production was significantly reduced during the last glacial period [e.g., *Boyle and Keigwin*, 1987; *Duplessy et al.*, 1988; *Sarnthein et al.*, 1994; *Curry and Oppo*, 2005]. Northern Component Waters (NCW) sank only to intermediate depth (<2000 m) forming Glacial North Atlantic Intermediate Water (GNAIW), extending from 45°N to 15°S. In contrast, it appears the production of water masses from the ACC (i.e., Southern Component Waters (SCW)) was either comparable to present day or increased with enhanced northward spreading, ventilating the deep North Atlantic below GNAIW [*Oppo and Fairbanks*, 1987; *Boyle and Keigwin*, 1987; *Marchitto and Broecker*, 2006].

[4] Paleoceanographic reconstructions of deep ocean variability in the South Atlantic have provided contrasting information on the relative influence of NADW and Antarctic Bottom Water (AABW) during the last glacial-interglacial cycle. Reduced production and southward spread of NADW during glacial periods has been suggested by studies using Nd isotope ratios [e.g., *Rutberg et al.*, 2000; *Piotrowski et al.*, 2004, 2005], $^{231}Pa/^{230}Th$ ratios in sediments [*McManus et al.*, 2004; *Gherardi et al.*, 2005], benthic $\delta^{13}C$ records [*Streeter and Shackleton*, 1979; *Sigman and Boyle*, 2000], and clay-mineral tracers [*Diekmann et al.*, 1996] which found that NCW extended no farther south than 40°S at the height of the last glacial period. In contrast, early studies using $^{231}Pa/^{230}Th$ ratios [*Yu et al.*, 1996] suggest that export of NCW to the Southern Ocean continued at a comparable rate to the Holocene during the Last Glacial Maximum (LGM), although probably at a reduced depth, a contention that also seems to be

[1] School of Earth, Ocean, and Planetary Sciences, Cardiff University, Cardiff, UK.
[2] Institució Catalana de Recerca i Estudis Avançats, Institut de Ciencia i Tecnología Ambientals, Universitat Autónoma de Barcelona, Bellaterra, Spain.

0883-8305/07/2006PA001407

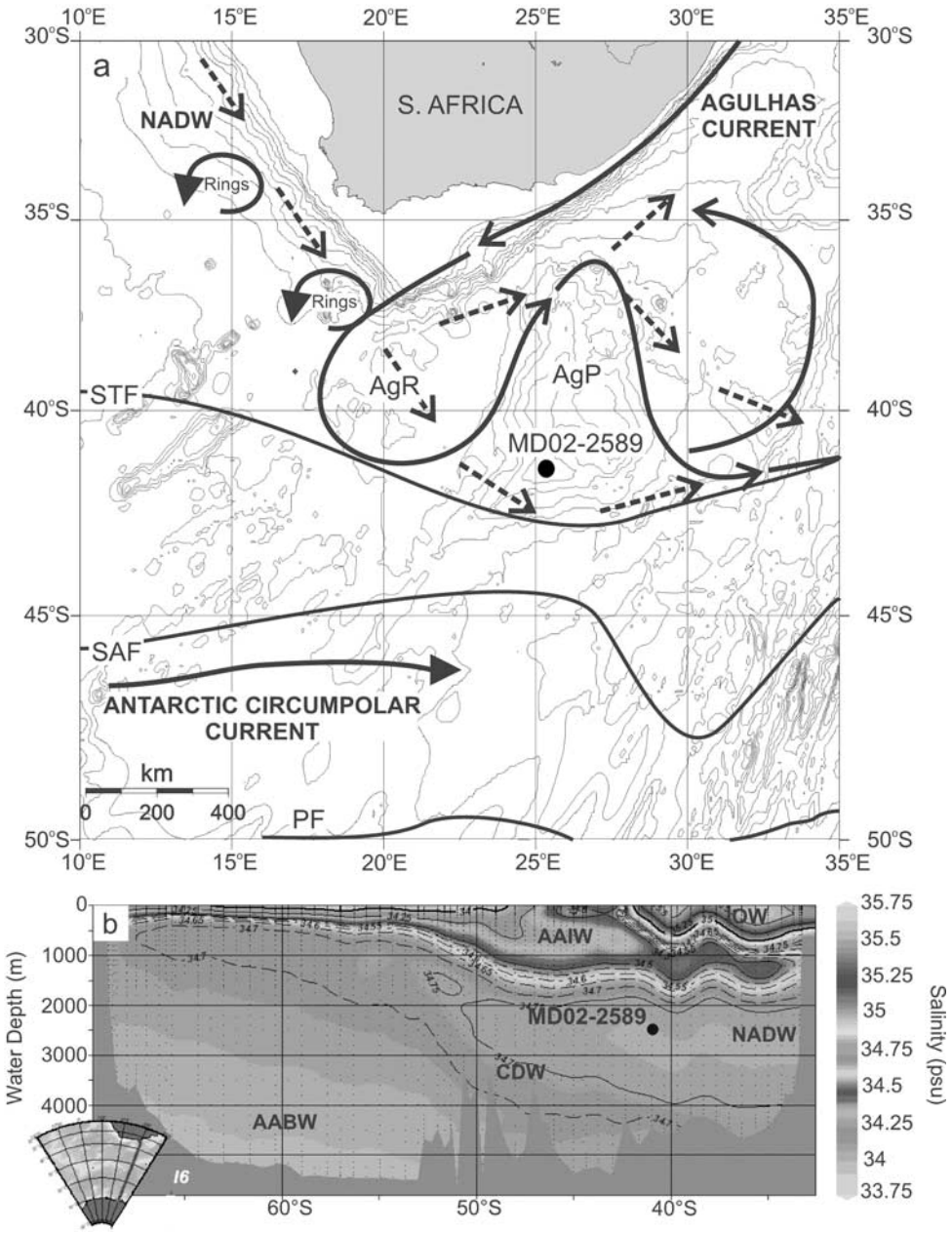

Figure 1. (a) Map showing study area and position of core MD02-2589 on the southern Agulhas Plateau, together with the present-day position of the oceanic fronts and generalised ocean circulation (after *Richardson et al.* [2003]). Position of the fronts after *Belkin and Gordon* [1996] and *Orsi et al.* [1995]. Solid arrows are surface water currents, and dashed arrows are bottom water currents. NADW, North Atlantic Deep Water; AgP, Agulhas Plateau; AgR, Agulhas Retroflection; STF, Subtropical Front; SAF, Subantarctic Front; PF, Polar Front. (b) Present-day transect of salinity from the coast of South Africa to Antarctica across the Southern Ocean (modified from *Schlitzer* [2000]) showing the positions of the existing water masses. IOW, Indian Ocean Water; AAIW, Antarctic Intermediate Water; NADW, North Atlantic Deep Water; CDW, Circumpolar Deep Water; AABW, Antarctic Bottom Water.

corroborated by Cd/Ca [*Boyle*, 1992; *Lea*, 1995] and foraminiferal isotope measurements in the southeast Pacific and Atlantic [*Matsumoto et al.*, 2001; *Matsumoto and Lynch-Stieglitz*, 1999]. Uncertainty is added to the picture by the indication of an expansion of SCW in two branches (Upper Southern Component Water and Lower Southern Component Water) that compensated for the suppression of NADW [*Henrich et al.*, 2003; *Curry and Oppo*, 2005] and a suggested presence of GNAIW in the Southern Ocean as a replacement for NADW [*Volbers and Henrich*, 2004]. *Bickert and*

Mackensen [2003] suggest that instead of GNAIW taking over from NADW, Mediterranean Outflow Water is more likely to have compensated but at a shallower depth and only certainly as far south as 30°S.

[5] The interhemispheric linkage of oceanic change has been the target of conceptual and numerical modeling [*Ganopolski and Rahmstorf*, 2001; *Seidov et al.*, 2001; *Weijer et al.*, 2002; *Knorr and Lohmann*, 2003; *Stocker and Johnsen*, 2003; *Weaver et al.*, 2003; *Knutti et al.*, 2004], while ice core synchronization exercises added insight from interhemispheric atmospheric paleodata comparisons that suggest an out-of-phase pattern between the hemispheres [*Blunier et al.*, 1998; *Blunier and Brook*, 2001; *Brook et al.*, 2005; *EPICA Community Members*, 2006]. The few high-resolution paleoceanographic records from the Southern Hemisphere oceans confirm this suggestion [*Charles et al.*, 1996; *Pahnke et al.*, 2003; *Pahnke and Zahn*, 2005], although such records are sparse and do not allow us to draw a conclusive picture for the wider Southern Hemisphere oceans. It has been suggested by early studies [*Hays et al.*, 1976; *Imbrie et al.*, 1989; *Howard and Prell*, 1992; *Labeyrie et al.*, 1996] that on orbital timescales, Southern Ocean sea surface temperatures (SST) respond early to changes in the orbital parameters and might actually lead global ice volume [*Charles et al.*, 1996]. The cause of such a lead is not well understood, as is the phasing of changes between the hemispheres on shorter suborbital timescales.

[6] Here we present a high-resolution multiproxy record of deep water variability from a sediment core recovered from the southern flank of the Agulhas Plateau in the southernmost South Atlantic. The location is close to the southern mixing interface between NADW and southern source waters in the Southern Ocean, enabling the reconstruction of the timing and amplitude of changes in southward advection of NADW and Southern Ocean THC. The site is also strongly influenced by the ACC. The flow of this current extends to depth, often to the seabed [*Orsi et al.*, 1995], and is wind driven, suggesting that fluctuations in the surface conditions can influence deep water dynamics. The position of the major frontal systems associated with the ACC can therefore be potentially related to changes in the near-bottom flow regime and strength. We concentrate on identifying the phasing between changes in ice volume, the location of surface ocean fronts, deep ventilation, and near-bottom flow speeds over the past 170 ka.

2. Regional Deep Water Oceanography

[7] The region connecting the Indian and Atlantic oceans (Figure 1) is one of several oceanic gateways guiding the flow of surface and deep waters around the global ocean and distributing heat, salt, and nutrients between the oceans [*Sloyan and Rintoul*, 2001; *Boebel et al.*, 2003]. Here deep water circulation is primarily characterized by the interactions between southward propagating NADW and northward flowing SCW, notably AABW and Antarctic Intermediate Water (AAIW) [*Reid*, 1989, 2005]. The transition between NADW and Lower Circumpolar Deep Water (LCDW) is at middepths sloping upward to the south (Figure 1b), while the deep areas (>5000 m) are filled with AABW, a mix of Weddell Sea Deep Water and LCDW [*Orsi et al.*, 1999].

[8] The interocean exchange of NADW into the South Indian Ocean from the South Atlantic occurs directly through the Agulhas Gateway, located between the southern tip of Africa and the northern Agulhas Plateau (Figure 1a). However, some of the NADW flow also extends toward the south, rounding the southern flank of the Agulhas Plateau where it has led to the deposition of contourite sediment drifts (Figure 1a) [*Tucholke and Carpenter*, 1977; *Uenzelmann-Neben*, 2001]. Core MD02-2589 (Figure 1) is positioned in a sediment drift up to 650 m thick that displays an asymmetric geometry and changes in internal reflector patterns which are indicative of a dynamical circulation pattern in the region back to Oligocene-Miocene times [*Uenzelmann-Neben*, 2002]. The core site today is predominantly bathed in NADW with a substantial Circumpolar Deep Water (CDW) contribution. The site thus offers the possibility to monitor past variations in CDW as a member of the Southern Ocean THC and the southward spreading of NADW.

3. Material and Methods

[9] Giant piston core MD02-2589 was recovered during R/V *Marion Dufresne* cruise MD128 from a contourite drift located on the southern Agulhas Plateau (41°26.03′S, 25°15.30′E, 2660 m water depth) (Figure 1a). At this depth the core site lies in NADW, ~1000 m below AAIW and ~1000 m above LCDW (Figure 1b). The core recovered 34.55 m of sediment, composed primarily of foraminiferal ooze, spanning the past ~1.3 Ma [*Giraudeau et al.*, 2002]. Here we focus on the upper 9.8 m of the sediment core, representing the last ~170 ka B.P. We sampled every 2 cm for stable isotope and grain-size analysis.

[10] The samples were first sieved to separate the fine (<63 μm) and coarse (>63 μm) fractions, with the fine fractions being used for grain-size analysis and the coarse fractions for isotope analysis. Epibenthic foraminiferal species *Fontbotia wuellerstorfi* (also commonly referred to as *Cibicidoides wuellerstorfi*), generally known to secrete calcite close to the $\delta^{13}C_{DIC}$ values of ambient bottom water [*Mackensen et al.*, 2001], was picked from the 150–250 μm size fraction. Eight to ten tests for each sample were analysed using a Finnigan MAT 252 mass spectrometer coupled with an automated Kiel III carbonate device. Long-term analytical precision is 0.06‰ for $\delta^{18}O$ and 0.03‰ for $\delta^{13}C$. All isotope data are referenced to the Vienna Peedee belemnite scale through repeated analysis of NBS 19 international carbonate standard. Oxygen isotopes of the benthic foraminifera *F. wuellerstorfi* have been transferred by +0.64‰ to the *Uvigerina spp.* scale as this more closely represents equilibrium with the ambient seawater [*Shackleton and Hall*, 1997].

[11] Grain-size analysis of the so-called sortable silt mean grain-size paleocurrent indicator uses the fraction of the sediment whose size sorting varies in response to hydrodynamic processes (i.e., the terrigenous 10–63 μm component) to infer relative changes in near-bottom current speed [*McCave et al.*, 1995a; *McCave and Hall*, 2006]. This proxy

Table 1. The ^{14}C AMS Ages on Planktonic Foraminifera and Calibrated Ages for Core MD02-2589

Lab Code	Depth, cm	Species[a]	Conventional ^{14}C Age, a	±1SD, a	Calibrated ^{14}C Age, a	±1SD, a
SUERC-4667[b]	5–6	*G. inflata*	13,161	±46	15,061	±102
SUERC-4668[b]	10–11	*G. inflata*	8,891	±29	9,505	±20
SUERC-4669[b]	20–21	*G. inflata*	11,731	±39	13,261	±103
SUERC-4670[b]	40–41	*G. inflata*	10,000	±33	10,954	±111
SUERC-4673	60–61	*G. inflata*	13,722	±50	15,874	±129
SUERC-4674	75–76	*G. inflata*	14,624	±53	17,181	±129
SUERC-4675	85–86	*G. inflata*	15,263	±57	18,230	±178
SUERC-4676	100–101	*G. inflata*	15,710	±60	18,603	±36
SUERC-4677	110–111	*G. inflata*	17,317	±73	20,137	±104
SUERC-4679	125–126	*G. inflata*	18,457	±84	21,538	±132
SUERC-4680	140–141	*G. inflata*	21,481	±120	25,288	±142
SUERC-4683	170–171	*G. inflata*	29,933	±335	34,664	±470
SUERC-4684	190–191	*G. inflata*	34,987	±628	39,927	±889

[a] *G.*, *Globorotalia*.
[b] Reversal and unused.

has been used successfully in paleocurrent studies in the North Atlantic [e.g., *Manighetti and McCave*, 1995; *Hall et al.*, 1998; *Bianchi and McCave*, 1999; *Ellison et al.*, 2006], South Atlantic [e.g., *Kuhn and Diekmann*, 2002], Indian [e.g., *McCave et al.*, 2005], and Pacific oceans [e.g., *Hall et al.*, 2001]. The samples were disaggregated in purified water on a rotating carousel for 24 h before being washed over a 63 μm mesh. Fine fraction residues were dried at 50°C, and carbonate was removed with 2 *M* acetic acid followed by digestion in 0.2% sodium carbonate at 80°C for 8 h to remove the biogenic silicates. Sortable silt mean ($\overline{SS}$) grain-size measurements were undertaken using a Coulter Multisizer III as detailed by *Bianchi et al.* [1999]. Average $\overline{SS}$ abundance in the samples is 8–10% enabling the determination of the $\overline{SS}$ index with an error of ±2% [*Bianchi et al.*, 1999].

[12] The degree of carbonate dissolution was assessed in selected samples using the planktonic foraminiferal fragmentation index described by *Le and Shackleton* [1992]. This index contains a devisor relating the number of fragments to the number of tests, so that percentage fragmentation is more likely to respond linearly to dissolution rather than being over sensitive during the early stages and relatively insensitive during the later stages of dissolution. Samples of the >150 μm size fraction were split as many times as required to obtain approximately 300 whole planktonic foraminifera. All whole planktonic foraminifera were identified and counted, while all fragments within these splits were also recorded. The percentage fragmentation was calculated using a fragment devisor of 3 [*Pfuhl and Shackleton*, 2004].

[13] A total of thirteen ^{14}C accelerator mass spectrometry (AMS) datings were carried out within the uppermost 190 cm of core MD02-2589 on monospecific samples containing ~1000 tests of *Globorotalia inflata* (Table 1). The ^{14}C analyses were carried out at the Natural Environment Research Council Radiocarbon Laboratory in East Kilbride, UK. The ^{14}C dates were corrected for the marine reservoir effect using a regional Southern Ocean correction of 800 years (a) [*Butzin et al.*, 2005] and subsequently calibrated to calendar years B.P. using the marine calibration data set of *Fairbanks et al.* [2005] which allows for calibration back to 50 ka.

4. MD02-2589 Chronology

[14] The age model for MD02-2589 was developed using a combination of AMS radiocarbon dating and graphic tuning of the benthic δ^{18}O records to core MD97-2120 [*Pahnke et al.*, 2003] (Figure 2) from the Chatham Rise, South Pacific. Two age reversals in the upper 60 cm of the core MD02-2589 led us to discard the four uppermost AMS dates (Table 1). Ages for this interval were estimated through extrapolation using a polynomial fit of the age/depth relationship of the remaining nine AMS dates (upper 190 cm). It should be noted that the ^{14}C calibrated ages appear typically older by ~1 ka from those derived by graphic correlation of the benthic δ^{18}O records of MD02-2589 and MD97-2120. Such an offset suggests that the local 800 a reservoir age that we have adopted for core MD02-2589 may well be an underestimate and reservoir ages rather are in the range of up to 1800 a, similar to those seen in MD97-2120 [*Pahnke et al.*, 2003] and other southwest Pacific Ocean sites [*Sikes et al.*, 2000]. Within the interval 190-982 cm (~40–170 ka), ages control points were assigned via graphic correlation of the benthic δ^{18}O with MD97-2120 (Figure 2) [*Pahnke et al.*, 2003]. The tuning of the benthic δ^{18}O records is further supported by the resulting close phase relationship of the planktonic δ^{18}O records of both cores, which show a high degree of synchronicity (not shown). The MD97-2120 age model is based on graphic correlations with both North Atlantic core MD95-2042 and Antarctic ice core Vostok δD record [*Pahnke et al.*, 2003]. MD97-2120 chosen as a reference to develop the age model for core MD02-2589 because it allowed direct correlation with Antarctic records as well as core MD95-2042 and other Northern Hemisphere climate records. The MD97-2120 benthic δ^{18}O profile has a similar structure to MD02-2589 especially over the MIS 5a/4 transition and in some of the smaller scale features thus facilitating the correlation (Figures 2a and 2b). Ages between each age control point were estimated by linear interpolation. The resulting age model suggests sedimenta-

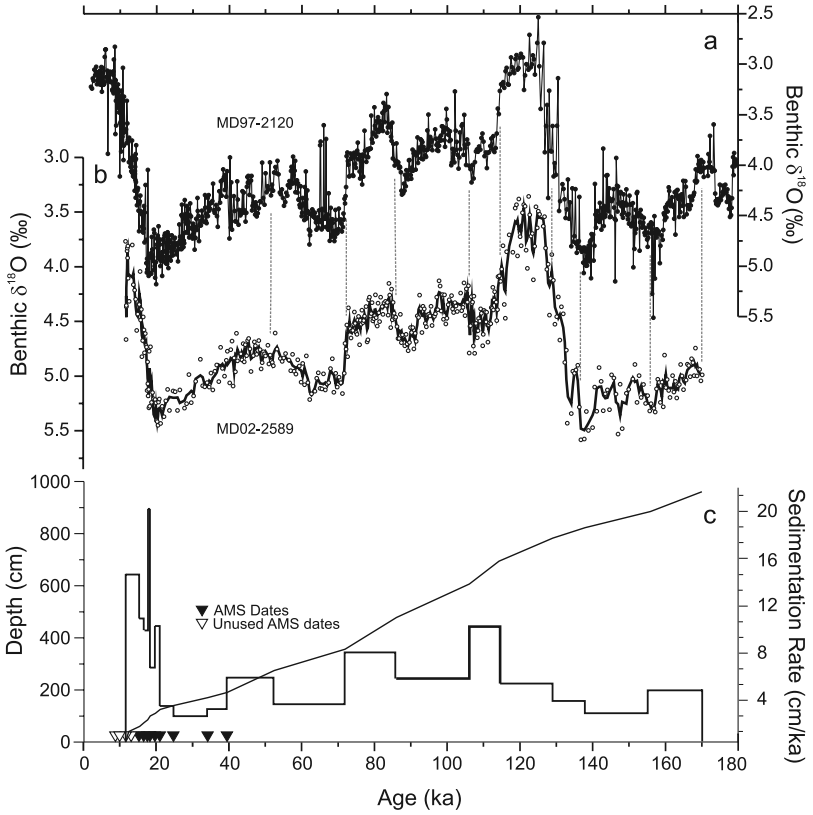

Figure 2. Chronology of core MD02-2589. (a) Benthic δ^{18}O record of core MD97-2120 [*Pahnke et al.*, 2003] and (b) benthic δ^{18}O record of MD02-2589, also showing tie points used for correlation, and (c) sedimentation rate and the position of both used and unused radiocarbon dates.

tion rates vary between ~15 cm ka^{-1} during glacials and ~5.5 cm ka^{-1} during interglacials (Figure 2c). At our 2 cm sampling resolution this equates to a mean time step along our proxy records of 298 ± 132 a.

5. Results

[15] The high-resolution benthic δ^{18}O record of MD02-2589 (Figure 3a) shows that orbital modulation caused by changing ice volume is the dominant control on this record. However, as the glacial-interglacial (G-I) benthic δ^{18}O amplitudes of the record (δ^{18}O ~2‰) are significantly greater than the shift associated with global ice volume changes (δ^{18}O 1–1.2‰ [*Schrag et al.*, 2002]) additional hydrographic changes in regional bottom water temperature and/or salinity are indicated over these timescales. The Holocene section in MD02-2589 is incomplete thus limiting our confidence in the reliability of the LGM to Holocene transition to assess the full G-I δ^{18}O shift at this location. As a result in the following discussion, only Termination II (TII) will be considered in detail. The benthic δ^{13}C record (Figure 3b) shows a G-I amplitude of ~0.8‰ ranging from values of −0.2–0‰ indicative of low ventilation during glacial stages MIS 6 and LGM, as well as MIS 4, to increased levels during warm stages MIS 5 and 3, with a more steady transition at TII than observed in the benthic δ^{18}O record. In contrast to the benthic δ^{18}O the benthic δ^{13}C values remain fairly consistent throughout MIS 5, with only modest orbital modulation, with minimum benthic δ^{13}C values occurring 5–7 ka after maximum benthic δ^{18}O associated with each cold substage. Conversely, benthic δ^{13}C shows clear evidence for millennial scale variability during MIS 3, which is not as apparent in the δ^{18}O record (Figure 3).

[16] The modern salinity distribution (Figure 1b) for the Agulhas sector of the Southern Ocean shows that site MD02-2589 lies in the southern extent of NADW close to where it merges with LCDW. Present-day NADW δ^{13}C in the South Atlantic typically has values of ~0.8‰ and LCDW is <0.5‰ [*Bickert and Wefer*, 1996]. A transect of late Holocene benthic δ^{13}C in the South Atlantic [*Mackensen et al.*, 2001] confirms that MD02-2589 (δ^{13}C ~0.65‰, Figure 3b) is currently positioned near the mixing zone between NADW and LCDW with the admixture of >50% NADW [e.g., *Bickert and Mackensen*, 2003]. Benthic δ^{13}C values in MIS 5 average 0.65‰ which again equates well with predicted δ^{13}C of NADW in the South Atlantic during interglacial periods (~0.6 − 0.7‰ [*Sarnthein et al.*, 1994]).

[17] The MD02-2589 $\overline{SS}$ record (Figure 3c) also reflects a distinctive orbital modulation, with higher values during glacial periods indicating enhanced near-bottom flow speeds. The amplitude of these G-I shifts in $\overline{SS}$ (G-I shift of 4 μm) are comparable to those seen at Ocean Drilling

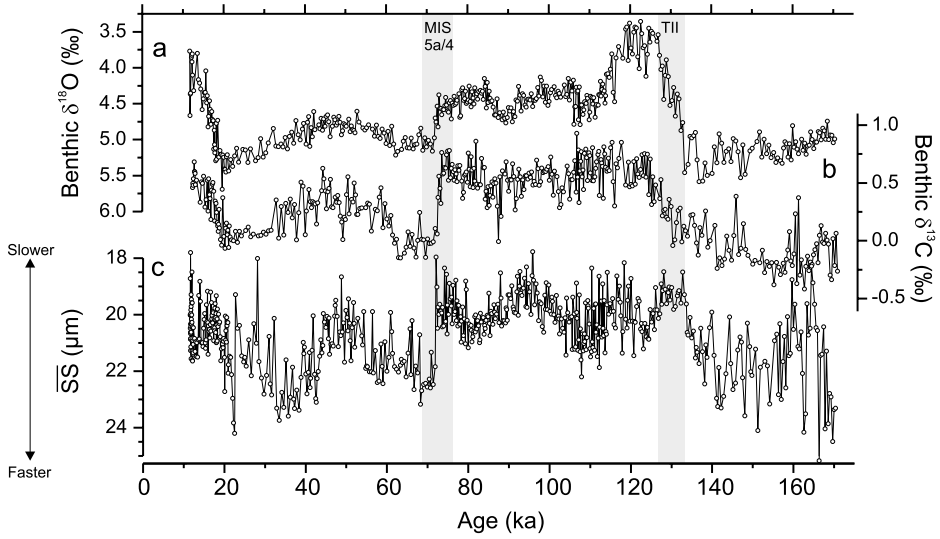

Figure 3. Benthic records of core MD02-2589 showing (a) benthic δ^{18}O, (b) benthic δ^{13}C, and (c) sortable silt mean grain size. Intervals focused on in this study are highlighted by the gray shading. MIS 5a/4, transition between marine oxygen isotope stages 5a and 4; TII, Termination II.

Program (ODP) Site 1123 in the SW Pacific (3–4 μm, [*Hall et al.*, 2001]) and core BOFS 6K from the East Thulean Rise, North Atlantic (3–4 μm, [*McCave et al.*, 1995b]). The modulation of $\overline{SS}$ within MIS 5 is offset from that seen in benthic δ^{18}O such that during the colder substages, MIS 5d and 5b flow speeds are in transition from low- to high-$\overline{SS}$ values reaching maximum values early in the following warm interval. While the $\overline{SS}$ record exhibits the highest degree of millennial scale variance throughout the entire interval, it is noticeable that within MIS 3, amplitudes of millennial scale variability in the δ^{13}C record are likewise increased and are substantially greater than those observed in the benthic δ^{18}O record (Figure 3). A complex temporal phasing across TII (and Termination I (TI)) is evident between each of the proxy records but the inferred flow speed changes and benthic δ^{13}C records are broadly negatively correlated on orbital timescales suggesting that periods of enhanced physical circulation ($\overline{SS}$) went along with reduced chemical ventilation (benthic δ^{13}C).

5.1. Glacial Terminations I and II

[18] At 141 ka, $\overline{SS}$ grain sizes at site MD02-2589 decrease rapidly coincident with the onset of a more gradual increase in benthic δ^{13}C, both preceding full glacial MIS 6.2 by some 3–4 ka (Figure 4). This initial reduction in flow speed and coeval onset of increasing ventilation occur some 8 ka before the start of the deglacial transition of TII at 133 ka (Figures 4d and 4f). Although hampered by the lack of Holocene recovery, the sequence of changes at TI suggests some differences from those occurring at TII (Figure 3). While an early decrease in flow speed and a low-flow speed plateau occurs within TI, in contrast to TII, benthic δ^{13}C appears to increase coincident with decreasing benthic δ^{18}O. This TI sequence and the lead of THC changes (ventilation and near-bottom flow speeds) over ice volume during TII in MD02-2589 is contrary to the sequence recently identified for TI by *Piotrowski et al.* [2005] suggesting a more complex phasing may be a feature of individual glacial terminations.

[19] The TII benthic δ^{13}C transition occurs in two steps. The initial intensification in ventilation, starting before the ice volume maximum at 141 ka, is gradual and only increases by 0.2‰ over 11 ka. This is followed by a larger and more rapid increase, starting at 130 ka, of 0.6‰ over 6 ka. Benthic δ^{13}C values also reach interglacial levels coincident with the δ^{13}C record of MD95-2042 and after the benthic δ^{18}O of MD02-2589 (Figure 4).

[20] The initial $\overline{SS}$ grain size decrease at 141 ka is halted by a reversal to faster near-bottom currents occurring between 139 and 138 ka coincident with the benthic δ^{18}O maximum. A more sustained flow speed decrease follows, reaching a period of prolonged low-flow speeds starting at 133 ka coincident with the start of TII in the benthic δ^{18}O record and lasting some 6 ka. A similar midtermination feature is seen in the benthic δ^{13}C records of RC11-83 and MD97-2120 during TII but intriguingly does not appear in the benthic δ^{13}C record of MD02-2589 (Figure 4).

5.2. MIS 5/4 Transition

[21] One of the most striking features seen in MD02-2589 records is the rapid transition between MIS 5a and MIS 4 (Figures 3 and 5). On the basis of our age model the transition starts at 73 ka from high benthic δ^{13}C values and low-flow speeds. The transition proceeds with a sharp transient increase in benthic δ^{18}O of 0.45‰ and decrease in benthic δ^{13}C of 0.4‰. Within 700 a of this excursion, flow speeds rapidly decrease reaching a minimum at 72 ka. An abrupt transition then occurs in all proxies reaching full MIS 4 conditions at 71.3 ka. The transition is led by increasing ice volume and followed by decreasing ventilation and then finally increasing flow speeds (Figure 5).

6. Discussion

[22] Temporal changes in benthic δ^{13}C at any location reflect some combination of the changes in the marine

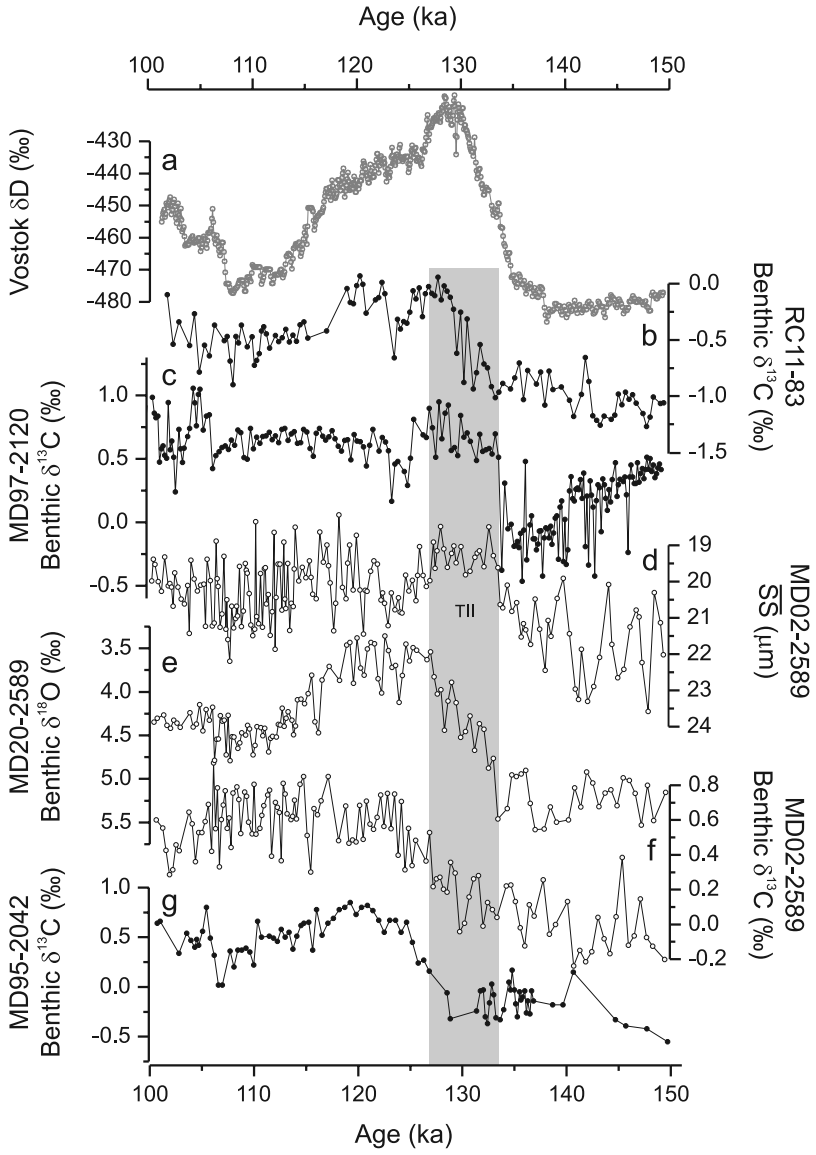

Figure 4. Southern Hemisphere records for Termination II. (a) Vostok δD [*Petit et al.*, 1999], (b) RC11-83 benthic δ^{13}C [*Charles et al.*, 1996], (c) MD97-2120 benthic δ^{13}C [*Pahnke and Zahn*, 2005], (d) MD02-2589 sortable silt mean grain size, (e) MD02-2589 benthic δ^{18}O, (f) MD02-2589 benthic δ^{13}C, and (g) MD95-2042 benthic δ^{13}C [*Shackleton et al.*, 2000]. Gray shading shows TII as indicated by MD02-2589 benthic δ^{18}O.

carbon reservoir, ocean circulation, air-sea gas exchange, and marine biological productivity [e.g., *Broecker and Maier-Reimer*, 1992; *Mackensen et al.*, 1993; *Lynch-Stieglitz and Fairbanks*, 1994; *Mackensen and Bickert*, 1999; *Oppo and Horowitz*, 2000] and have traditionally been a tool with which to trace deep water masses. [e.g., *Streeter and Shackleton*, 1979; *Sigman and Boyle*, 2000; *Bostock et al.*, 2004]. In the South Atlantic, high δ^{13}C signatures signify young, nutrient-depleted, well-ventilated North Atlantic Deep Waters, while lower increasingly negative δ^{13}C values are linked to older, nutrient-enriched Antarctic water masses which have reduced ventilation due to long isolation from the atmosphere. Fluctuations in δ^{13}C in this region are linked to variations in the proportion of better ventilated NCW versus lesser ventilated SCW. The mean grain size of the 10–63 μm size fraction ($\overline{\text{SS}}$) responds linearly to changes in flow conditions 20–100 m above the bed [*McCave et al.*, 1995b], with higher grain sizes denoting faster flow and vice versa. The region south of $\sim$40°S in the Southern Ocean is dominated by the ACC, with changes in $\overline{\text{SS}}$ plausibly reflecting variations in the strength of its flow. The ACC flow is driven by surface wind forcing which may affect the whole water column through frictional effects down to deeper depths [*Orsi et al.*, 1995] and is therefore linked into Southern Hemisphere climate change, as is the expansion and contraction of the surface ocean fronts. However, the strengthening and weakening of the ACC can also therefore be possible

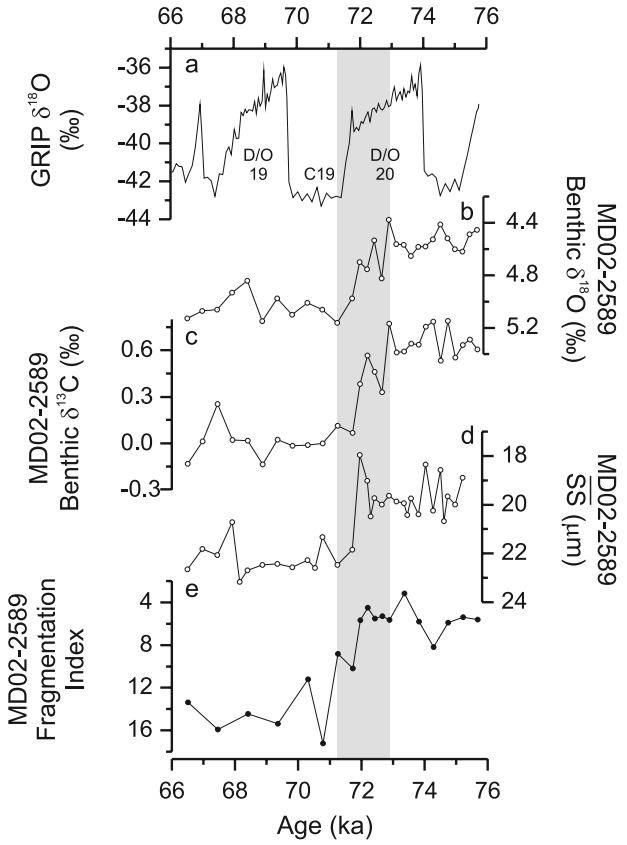

Figure 5. Proxy records of the MIS 5a-4 transition. (a) GRIP $\delta^{18}O$ [*Johnsen et al.*, 1997], (b) MD02-2589 benthic $\delta^{18}O$, (c) MD02-2589 benthic $\delta^{13}C$, (d) MD02-2589 sortable silt mean grain size, and (e) MD02-2589 fragmentation index. Gray shading shows the transition as defined in the text. D/O, Dansgaard-Oeschger events; C19, Greenland event [*McManus et al.*, 1994].

without frontal movements. These differences in tracer signals allow a decoupling of flow speed and water mass provenance at certain sites, which can be explained by changes in different components of a mixed water mass affecting either provenance or flow speed in different ways.

[23] The export of NCW from the North Atlantic during glacial periods is poorly constrained and has been discussed controversially in literature [e.g., *Sarnthein et al.*, 1994; *Yu et al.*, 1996; *Matsumoto et al.*, 2001; *Curry and Oppo*, 2005]. In order to identify the NCW influence at the MD02-2589 site during glacial periods we compare our data with several existing benthic $\delta^{13}C$ records. For this comparison we have chosen deep South Atlantic cores RC11-83 [*Charles et al.*, 1996] and TN057-21 (Table 2 [*Ninnemann and Charles*, 2002]), which remained strongly influenced by SCW (i.e., AABW) over both glacial and interglacial periods. We also use core MD97-2120 (Table 2 [*Pahnke and Zahn*, 2005]) from the Chatham Rise, southwest Pacific, as an alternative Southern Ocean record documenting AAIW variability. Finally, core MD95-2042 (Table 2 [*Shackleton et al.*, 2000]) from the Iberian Margin was chosen as a North Atlantic reference as it is high resolution, has a timescale that has been tied to both Vostok and Greenland Ice Core Project (GRIP) and reflects changing northern versus southern water sources in the North Atlantic during glacial periods.

[24] Offsets in amplitude of the benthic $\delta^{18}O$ G-I shifts between MD02-2589 and sites RC11-83, MD97-2120, and MD95-2042 (Figure 6) plausibly reflect differences in *T-S* changes of water masses bathing each site. Average glacial benthic $\delta^{18}O$ values at site MD02-2589 are between 0.3–0.7‰ heavier than average glacial values in cores from the South Atlantic (core RC11-83), North Atlantic (core MD95-2042), and SW Pacific (core MD97-2120) (Figure 6), suggesting that deep water at the Agulhas Plateau during the last two glacial periods was colder or saltier (or a combination of both) than deep waters in the North Atlantic and intermediate water in the southwest Pacific. Assuming that deep ocean temperature in the glacial ocean was uniformly colder and presumably close to the freezing point of seawater [*Waelbroeck et al.*, 2002; *Adkins et al.*, 2002], this makes seawater $\delta^{18}O$ and thus salinity the most plausible candidates to have caused the observed offsets in benthic $\delta^{18}O$, although there was probably a very different salinity-$\delta^{18}O$ relationship during glacial periods than in modern day. *Adkins et al.* [2002] and *Adkins and Schrag* [2003] suggest that the Southern Ocean had the saltiest LGM deep water due to increased sea-ice formation. As sea-ice formation offsets seawater $\delta^{18}O$ from its global correlation with salinity, some of the offset in benthic $\delta^{18}O$ seen in Figure 4 may reflect the contribution of these Southern Ocean deep waters to the deeper core sites, namely RC11-83, which at 4600 m water depth and at a location close to the Southern Ocean most likely records modified AABW.

[25] The mean ocean shift of $\delta^{13}C$ in seawater ΣCO_2 between the LGM and Holocene has been estimated to be between 0.32‰ [*Duplessy et al.*, 1988] and 0.46‰ [*Curry et al.*, 1988]. The benthic $\delta^{13}C$ G-I shift observed in MD02-2589 of 0.8‰ (Termination II Figure 3b) suggests an additional 0.3–0.4‰ variation in $\delta^{13}C$ must be explained by varying water masses, surface productivity changes, and/or air-sea exchange processes. This additional 0.3–0.4‰ $\delta^{13}C$ G-I variation is 20–40% less than the benthic $\delta^{13}C$ shift of 0.5‰ predicted for a complete halt of NCW advection to the south [*Charles et al.*, 1996]. The reduced

Table 2. Station Data for Cores Used in This Study

Core	Latitude	Longitude	Depth, m	Reference
MD02-2589	41°19′S	25°15′E	2660	This study
RC11-83	41°36′S	9°48′E	4718	*Charles et al.* [1996]
TN057-21	41°08′S	7°49′E	4981	*Ninnemann and Charles* [2002]
MD97-2120	45°32′S	174°55′E	1210	*Pahnke and Zahn* [2005]
MD95-2042	37°48′N	10°10′W	3146	*Shackleton et al.* [2000]

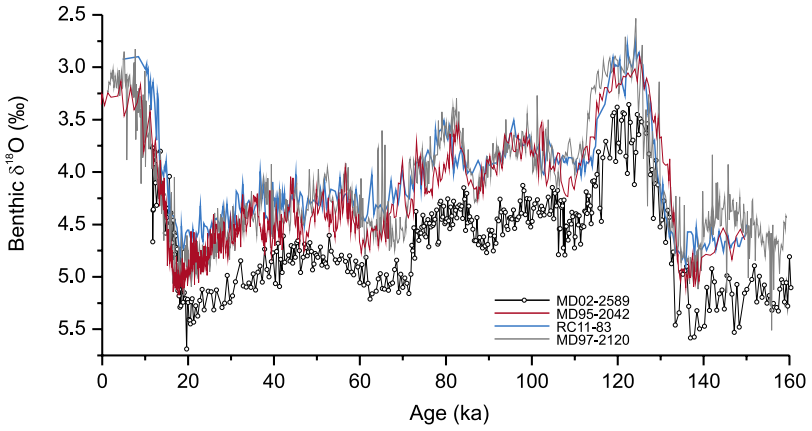

Figure 6. Records of benthic $\delta^{18}O$ of *Fontbotia wuellerstorfi* from MD02-2589, RC11-83 [*Charles et al.*, 1996], MD97-2120 [*Pahnke et al.*, 2003], and MD95-2042 [*Shackleton et al.*, 2000]. All data are shown on the Uvigerina scale.

$\delta^{13}C$ shift observed in MD02-2489 therefore indicates a persistent contribution of a well-ventilated water mass to the ambient glacial bottom waters with a $\delta^{13}C$ signature similar to present-day NCW. This can either be explained as sustained NCW influence at the site over the past 170 ka or the presence of SCW exhibiting a similar $\delta^{13}C$ signature from air-sea gas exchanges. Studies have suggested that during glacial periods, enhanced production of deep waters occurred in the zone of extended winter sea ice coverage (out to ~50°S) south of the Polar Front (PF) [*Rosenthal et al.*, 1997; *Mackensen et al.*, 2001; *Bickert and Mackensen*, 2003] and as a second shallower deep water mass along the Subantarctic Front (SAF) [*Michel et al.*, 1995]. If any of these scenarios holds true, the proximity of site MD02-2589 to the SAF would bring it under the influence of this shallower water mass during glacial periods. Benthic $\delta^{13}C$ of *F. wuellerstorfi* in MD02-2589 remains consistently more positive by ~0.7‰ than that in the deeper AABW-influenced cores RC11-83 and TN057-21(Figure 7) further providing evidence for a consistently better ventilation of middepth isopycnals. Benthic $\delta^{13}C$ from cores located in the deeper Cape Basin [*Charles and Fairbanks*, 1992; *Bickert and Wefer*, 1999] and carbonate dissolution in the Cape and Angola basins inferred from sand contents [*Bickert and Wefer*, 1996] were used previously to infer reduced NADW advection to the south leading to a reduced contribution to or even complete absence of NCW in the deep glacial Southern Ocean. On the basis of our data we conclude that this scenario may not hold for the high-latitude South Atlantic as a whole but that a better ventilated water mass must have been present at middepth. This is further suggested in a study by *Hodell et al.* [2003] based on a vertical transect of benthic $\delta^{13}C$ at the Agulhas Ridge, which suggests the presence of a well-developed chemocline in the South Atlantic at the LGM with a sharp chemical divide

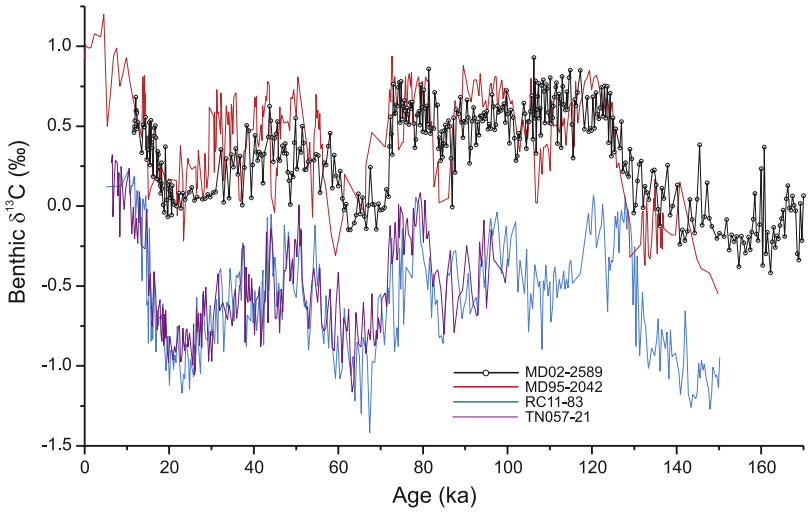

Figure 7. Records of benthic $\delta^{13}C$ of *Fontbotia wuellerstorfi* from MD02-2589, RC11-83 [*Charles et al.*, 1996], TN057-21 [*Ninnemann and Charles*, 2002], and MD95-2042 [*Shackleton et al.*, 2000].

between well-ventilated middepth waters above 2500 m and less well-ventilated deep waters below.

[26] *Hall et al.* [2001] found $\overline{SS}$ grain sizes at ODP Site 1123 in the SW Pacific were coherent with both benthic $\delta^{18}O$ and $\delta^{13}C$ isotopes at each orbital frequency. A clear relationship was also seen between $\overline{SS}$ and the Pacific deep water $\delta^{13}C$ aging trends ($\Delta\delta^{13}C$ ODP Sites 1123–849) with periods of decreased aging inferred from isotopes associated with increased Deep Western Boundary Current (DWBC) flow speeds (physical ventilation). *Hall et al.* [2001] concluded that such flow changes may be directly related to increased production of AABW during the glacials potentially controlled by Southern Ocean winds or greater annual production of sea ice leading to water densification through brine rejection. A similar orbital scale relationship between benthic $\delta^{13}C$ and changing near-bottom flow speeds is observed in the MD02-2589 records, with decreased benthic $\delta^{13}C$ and increased near-bottom flow speeds during glacial periods. However, given that benthic $\delta^{13}C$ at MD02-2589 suggests better ventilation at middepths (compared to bottom water sites), additional controls on physical ventilation are indicated. The total transport of the ACC is thought to be around 130 sverdrup (10^6 m^3 s^{-1}) [*Whitworth and Peterson*, 1985; *Cunningham et al.*, 2003] with the bulk of this transport occurring within deep-reaching narrow jets at the PF and SAF, at a mean water depth of 3000 m [*Nowlin and Klinck*, 1986; *Gille*, 1994; *Orsi et al.*, 1995]. At the present-day, MD02-2589 lies to the north of both the PF and SAF (by ~8° and ~3°, respectively [*Belkin and Gordon*, 1996; *Anilkumar et al.*, 2005]) and therefore outside the immediate ACC. Increased flow speeds during glacial periods (Figure 3c), however, imply that both mobile surface ocean fronts shifted to the north [*Mackensen et al.*, 2001; *Hays et al.*, 1976; *Burckle*, 1984; *Pudsey and Howe*, 1998]. Thus MD02-2589 plausibly came within the reach of the ACC and its faster flowing deep current jets during glacial periods that presumably restricted the southward transports of northern source deep waters deep into the Southern Ocean. Better ventilation of ambient bottom waters at the core site, in this case, would more clearly support a contribution of a Southern Ocean water mass with a ventilation signature influenced by air-sea gas exchange, similar to that seen in AAIW today.

6.1. Glacial Termination

[27] *Bianchi and Gersonde* [2002] describe a southward displacement of the edge of the winter sea ice and a sea surface temperature warming in the Atlantic and western Indian Antarctic Zone, prior to MIS 5e, during late MIS 6 that was followed by a southward shift of the PF by 3–5° latitude from its current position during the late termination. The increase in ventilation displayed in the benthic $\delta^{13}C$ record of core RC11-83 and MD97-2120 and the sustained decrease in flow speeds at MD02-2589 starting at ~138 ka (Figure 4) likely correspond to this SST warming. Minimum flow speeds at MD02-2589 and maximum benthic $\delta^{13}C$ values in RC11-83 and MD97-2120 (Figure 4) coincide with the southward shift of the PF. Evidence for warming within the region during late MIS 6 and a climate optimum within the glacial termination has recently been shown by faunal records of *Peeters et al.* [2004] from the South African margin which suggest that following the arrival of the Subtropical Front at its most northerly location during peak MIS 6, it started to move southward well before the start of the termination allowing increased leakage through the Indian-Atlantic surface throughflow area that reaches a maximum within TII (also seen in modeling evidence of *Knorr and Lohmann* [2003]). Additionally, a sea level record from the Red Sea [*Siddall et al.*, 2006] shows a highstand during TII which lasted several millennia, followed by a reversal of 30 to 40 ± 12 m coincident with the early warming of the southern latitudes. Correlating the benthic $\delta^{18}O$ shifts and circulation proxy changes in cores MD02-2589 and MD97-2120 [*Pahnke et al.*, 2003] with the Vostok ice core, suggests that the prominent δD peak in Vostok that is indicative of peak maximum air temperatures over Antarctica [*Petit et al.*, 1999] (and EPICA Dome C records [*Jouzel et al.*, 2004]) occurred prior to full-interglacial MIS 5e during mid-TII (Figure 4), although age model constraints do not currently allow us to further address this possibility.

[28] The climate optimum within the transition is followed by a marked cooling at around 128 ka, seen in Vostok δD, and is coincident with an increase in flow speed at MD02-2589, a decrease in ventilation at RC11-83 and MD97-2120 (Figure 4), and a southern high-latitude-wide SST cooling and expansion of the winter sea ice limit [*Bianchi and Gersonde*, 2002]. The cooling of the Antarctic continent evident in the Vostok δD record has been linked with an intensification of Northern Hemisphere deep water to full interglacial levels [*Sarnthein and Tiedemann*, 1990; *Diekmann et al.*, 1996; *Spero and Lea*, 2002], a suggestion that is supported by the benthic $\delta^{13}C$ record of MD02-2589 which show an increase in ventilation during this event reaching maximum levels at around 124 ka. Given the benthic $\delta^{18}O$ record of MD02-2589 suggests that the onset of MIS 5e occurs at 127 ka (Figure 4), then this period of increased flow speeds and ventilation at Agulhas Plateau and the wider Southern Hemisphere cooling occurs during the earliest part of the full interglacial.

[29] From the above we conclude that during TII, changes in chemical ventilation, related to the southward advection of NCW, are largely decoupled at site MD02-2589 from near-bottom physical flow speeds that primarily relate to the expansion and contraction of the ACC in association with meridional movements of the PF and SAF.

6.2. MIS 5/4 Transition

[30] The MIS 5a/4 transition starts at 73 ka from benthic $\delta^{13}C$ values indicative of maximum NCW influence and low-flow speed values suggestive of weakened ACC flow (Figures 3 and 5). This supports the suggestion by *Peeters et al.* [2004] for a strong input of NADW to the Southern Ocean associated with an abundance peak in Agulhas leakage fauna, observed in core MD01-2081, before the MIS 5a/4 transition recorded in its associated benthic $\delta^{18}O$ record and plausibly interpreted as a westward propagation of the Agulhas Current and an enhanced Indian-Atlantic surface transport.

[31] The changes observed in $\overline{SS}$ and benthic $\delta^{13}C$ at the transition are similar in magnitude to the opposite trends seen during the TII glacial-interglacial shifts. The MIS 5a/4 benthic $\delta^{13}C$ shift (~0.9‰) is also similar in magnitude to those observed in deep AABW-influenced cores TN057-21 and RC11-83 (~0.95‰). Although a significant portion of the MIS 5a/4 benthic $\delta^{13}C$ shift is likely due to a change in the carbon reservoir signal [*Piotrowski et al.*, 2005], as MIS 4 constitutes full glacial conditions for the first time after the prolonged interglacial conditions of MIS 5, these data along with the near-bottom flow speeds suggest a decrease in NADW influence and an expansion of the SCW over the Agulhas Plateau.

[32] This switch in water mass influence is consistent with a coeval transition in the MD02-2589 record from low fragmentation percentage, indicative of a carbonate saturated water mass sustaining higher levels of carbonate preservation (e.g., NCW), to high fragmentation percentage, indicative of a carbonate undersaturated water mass more corrosive to carbonates (e.g., SCW) [*Henrich et al.*, 2003; *Pfuhl and Shackleton*, 2004]) (Figure 5e). In addition, records from ODP Site 1059 (32.1°N, 76.4°W, 2584 m water depth) and 1057 (31.40°N, 75.25°W, 2985 m water depth) from the Blake Outer Ridge (BOR), North Atlantic [*Evans et al.*, 2007], show a sharp, short-lived, negative excursion in benthic $\delta^{13}C$ over the sites at 73.2 ka and 71.6 ka, respectively, during the transition in their associated benthic $\delta^{18}O$ records, which is attributed to an abrupt shoaling (to <2500 m) of the DWBC at the BOR associated with a reduction in production of NADW, at the MIS 5a/4 transition. The GRIP ice core $\delta^{18}O$ record from Greenland [*Johnsen et al.*, 1997] also exhibits a significant cold event (C19 in contemporaneous marine cores [*McManus et al.*, 1994]) at 71.5 ka (Figure 5). Neodymium isotope analysis on cores RC11-83 and TN057-21 [*Piotrowski et al.*, 2005] also confirm this event, showing a rapid decrease in the proportion of NADW in bottom water over this transition.

7. Conclusions

[33] Our high-resolution benthic $\delta^{13}C$ record from core MD02-2589 strongly suggests that there was a continued source for enhanced middepth ventilation over the southern Agulhas Plateau during glacial periods. While the influence of NCW may have been reduced in the glacial South Atlantic, additional well-ventilated waters plausibly have originated in the Southern Ocean. Significantly increased near-bottom flow speeds during glacial periods at MD02-2589 indicate that the vigor of near-bottom currents on the southern Agulhas Plateau is likely influenced by orbital scale meridional expansion and contraction of the ACC and its associated surface fronts.

[34] Ventilation and flow speeds show a late MIS 6 circulation change, associated with the previously documented [e.g., *Bianchi and Gersonde*, 2002] regional frontal shifts and SST warming in the Southern Ocean, occurring some 8 ka before the start of TII recorded in the benthic $\delta^{18}O$. A mid-TII climate optimum is highlighted in the MD02-2589 record by a transient episode of low-flow speeds concurrent with a period of increased ventilation shown in the benthic $\delta^{13}C$ records from other cores from Southern Ocean deep (RC11-83) and intermediate (MD97-2120) sites. This event is not recorded in the benthic $\delta^{13}C$ of MD02-2589.

[35] All of the MD02-2589 records show a rapid, but sequenced, event occurring at the MIS 5a/4 transition, in which changes in flow speed and chemical ventilation were of a similar magnitude (but opposite direction) to those occurring at TII. These changes suggest a switch in the relative influence of northern and southern source waters, together with an increased influence of the ACC, toward MIS 4. This event can be linked to the sudden shoaling of NADW and reduction in its production possibly related to GRIP 2 cold event C19.

[36] **Acknowledgments.** We are grateful to G.G. Bianchi, J. Becker, and H. Medley for assistance with sample preparation and analysis. E.M. and I.H. acknowledge support by the Natural Environment Research Council (NERC) and the NERC Radiocarbon Laboratory, UK. R.Z. acknowledges support from the Ministerio de Educacion y Ciencias, Spain. We would also like to thank A.M. Piotrowski, E. Michel, B. Diekmann, and an anonymous reviewer for their constructive reviews and comments which greatly improved this manuscript. G. Martinez-Mendez, Universitat Autònoma de Barcelona, provided her insight into the paleoceanography of the Agulhas Corridor region. We thank the Institut Polaire Français Paul Emile Victor for technical support and for making the R/V *Marion Dufresne* available and J. Giraudeau and Y. Balut for their support in recovering this core.

References

Adkins, J. F., and D. P. Schrag (2003), Reconstructing Last Glacial Maximum bottom water salinities from deep-sea sediment pore fluid profiles, *Earth Planet. Sci. Lett.*, *216*, 109–123.

Adkins, J. F., K. McIntyre, and D. P. Schrag (2002), The salinity, temperature, and $\delta^{18}O$ of the glacial deep ocean, *Science*, *298*, 1769–1773.

Anilkumar, N., M. K. Dash, A. J. Luis, V. Ramesh Babu, Y. K. Somayajulu, M. Sudhakar, and P. C. Pandey (2005), Oceanic fronts along 45°E across Antarctic Circumpolar Current during austral summer 2004, *Curr. Sci.*, *88*, 1669–1673.

Belkin, I. M., and A. L. Gordon (1996), Southern Ocean fronts from the Greenwich meridian to Tasmania, *J. Geophys. Res.*, *101*, 3675–3696.

Bianchi, C., and R. Gersonde (2002), The Southern Ocean surface between Marine Isotope Stages 6 and 5d: Shape and timing of climate changes, *Palaeogeogr. Palaeoclimatol. Palaeoecol.*, *187*, 151–177.

Bianchi, G. G., and I. N. McCave (1999), Holocene periodicity in North Atlantic climate and deep-ocean flow south of Iceland, *Nature*, *397*, 515–517.

Bianchi, G. G., I. R. Hall, I. N. McCave, and L. Joseph (1999), Measurement of the sortable silt current speed proxy using the Sedigraph 5100 and Coulter Multisizer IIe: Precision and accuracy, *Sedimentology*, *46*, 1001–1014.

Bickert, T., and A. Mackensen (2003), Last glacial to Holocene changes in South Atlantic deep water circulation, in *The South Atlantic in the Late Quaternary: Reconstruction of Material Budgets and Current Systems*, edited by G. Wefer, S. Mulitza, and V. Ratmeyer, pp. 671–695, Springer-Verlag, Berlin.

Bickert, T., and G. Wefer (1996), Late Quaternary deep water circulation in the South Atlantic: Reconstruction from carbonate dissolution and benthic stable isotopes, in *The South Atlantic: Present and Past Circulation*, edited

by G. Wefer et al., pp. 599–620, Springer-Verlag, Berlin.

Bickert, T., and G. Wefer (1999), South Atlantic and benthic foraminifer $\delta^{13}C$ deviations: Implications for reconstructing the late Quaternary deep-water circulation, *Deep Sea Res. Part II*, *46*, 437–452.

Blunier, T., and E. J. Brook (2001), Timing of millennial-scale climate change in Antarctica and Greenland during the last glacial period, *Science*, *291*, 109–112.

Blunier, T., et al. (1998), Asynchrony of Antarctic and Greenland climate change during the last glacial period, *Nature*, *394*, 739–743.

Boebel, O., J. Lutjeharms, C. Schmid, W. Zenk, T. Rossby, and C. Barron (2003), The Cape Cauldron: A regime of turbulent inter-ocean exchange, *Deep Sea Res. Part II*, *50*, 57–86.

Bostock, H. C., B. N. Opdyke, M. K. Gagan, and L. K. Fifield (2004), Carbon isotope evidence for changes in Antarctic Intermediate Water circulation and ocean ventilation in the southwest Pacific during the last deglaciation, *Paleoceanography*, *19*, PA4013, doi:10.1029/2004PA001047.

Boyle, E. A. (1992), Cadmium and $\delta^{13}C$ paleochemical ocean distributions during the stage 2 glacial maximum, *Annu. Rev. Earth Planet. Sci.*, *20*, 245–287.

Boyle, E. A., and L. D. Keigwin (1987), North Atlantic thermohaline circulation during the past 20,000 years linked to high-latitude surface temperature, *Nature*, *330*, 35–40.

Broecker, W. S., and E. Maier-Reimer (1992), The influence of air and sea exchange on the carbon isotope distribution in the sea, *Global Biogeochem. Cycles*, *6*, 315–320.

Brook, E. J., J. W. C. White, A. S. M. Schilla, M. L. Bender, B. Barnett, J. P. Severinghaus, K. C. Taylor, R. B. Alley, and E. J. Steig (2005), Timing of millennial-scale climate change at Siple Dome, West Antarctica, during the last glacial period, *Quat. Sci. Rev.*, *24*, 1333–1343.

Burckle, L. H. (1984), Diatom distribution and paleogeographic reconstruction in the Southern Ocean: Present and Last Glacial Maximum, *Mar. Micropaleontol.*, *9*, 241–261.

Butzin, M., M. Prange, and G. Lohmann (2005), Radiocarbon simulations for the glacial ocean: The effects of wind stress, Southern Ocean sea ice, and Heinrich events, *Earth Planet. Sci. Lett.*, *235*, 45–61.

Charles, C. D., and R. G. Fairbanks (1992), Evidence from Southern Ocean sediments for the effect of North Atlantic deep-water flux on climate, *Nature*, *355*, 416–419.

Charles, C. D., J. Lynch-Stieglitz, U. S. Ninnemann, and R. G. Fairbanks (1996), Climate connections between the hemisphere revealed by deep sea sediment core/ice core correlations, *Earth Planet. Sci. Lett.*, *142*, 19–27.

Cunningham, S. A., S. G. Alderson, B. A. King, and M. A. Brandon (2003), Transport and variability of the Antarctic Circumpolar Current in Drake Passage, *J. Geophys. Res.*, *108*(C5), 8084, doi:10.1029/2001JC001147.

Curry, W. B., and D. W. Oppo (2005), Glacial water mass geometry and the distribution of $\delta^{13}C$ of ΣCO_2 in the western Atlantic Ocean, *Paleoceanography*, *20*, PA1017, doi:10.1029/2004PA001021.

Curry, W. B., J.-C. Duplessy, L. Labeyrie, and N. J. Shackleton (1988), Changes in the distribution of $\delta^{13}C$ of deep water ΣCO_2 between the last glaciation and the Holocene, *Paleoceanography*, *3*, 317–341.

de Ruijter, W. P. M., A. Biastoch, S. S. Drijfhout, J. R. E. Lutjeharms, R. P. Matano, T. Pichevin, P. J. van Leeuwen, and W. Weijer (1999), Indian-Atlantic interocean exchange: Dynamics, estimation and impact, *J. Geophys. Res.*, *104*, 20,885–20,910.

Diekmann, B., R. Petschick, F. X. Gingele, D. K. Futterer, A. Abelmann, U. Brathauer, R. Gersonde, and A. Mackensen (1996), Clay mineral fluctuations in late Quaternary sediments of the southeastern South Atlantic: Implications for past changes in deep water advection, in *The South Atlantic: Present and Past Circulation*, edited by G. Wefer et al., pp. 621–644, Springer-Verlag, Berlin.

Duplessy, J.-C., N. J. Shackleton, R. G. Fairbanks, L. Labeyrie, D. Oppo, and N. Kallel (1988), Deepwater source variations during the last climatic cycle and their impact on the global deepwater circulation, *Paleoceanography*, *3*, 343–360.

Ellison, C. R. W., M. R. Chapman, and I. R. Hall (2006), Surface and deep ocean interactions during the cold climate event 8200 years ago, *Science*, *312*, 1929–1932.

EPICA Community Members (2006), One-to-one hemispheric coupling of millennial polar climate variability during the last glacial, *Nature*, *444*, 195–198.

Evans, H. K., I. R. Hall, G. G. Bianchi, and D. W. Oppo (2007), Intermediate water links to Deep Western Boundary Current variability in the subtropical NW Atlantic during marine isotope stages 5 and 4, *Paleoceanography*, *22*, PA3209, doi:10.1029/2006PA001409.

Fairbanks, R. G., R. A. Mortlock, T.-C. Chiu, L. Cao, A. Kaplan, T. P. Guilderson, T. W. Fairbanks, A. L. Bloom, P. M. Grootes, and M.-J. Nadeau (2005), Radiocarbon calibration curve spanning 0 to 50,000 years BP based on paired 230Th/234U/238U and 14C dates on pristine corals, *Quat. Sci. Rev.*, *24*, 1781–1796.

Ganopolski, A., and S. Rahmstorf (2001), Rapid changes of glacial climate simulated in a coupled climate model, *Nature*, *409*, 153–158.

Gherardi, J. M., L. Labeyrie, J. F. McManus, R. Francois, L. C. Skinner, and E. Cortijo (2005), Evidence from the northeastern Atlantic basin for variability in the rate of the meridional overturning circulation through the last deglaciation, *Earth Planet. Sci. Lett.*, *240*, 710–723.

Gille, S. T. (1994), Mean sea surface height of the Antarctic Circumpolar Current from Geosat data: Method and application, *J. Geophys. Res.*, *99*(C9), 18,255–18,273.

Giraudeau, J., R. Zahn, and I. R. Hall (2002), Agulhas current variability: Calypso long sediment coring off South Africa, cruise report R/V Marion Dufresne cruise MD128, Dept. of Geol. and Oceanogr., Univ. of Bordeaux, Talence, France.

Gordon, A. L. (1996), Comment of the South Atlantic's role in the global circulation, in *The South Atlantic: Present and Past Circulation*, edited by G. Wefer et al., pp. 121–124, Springer-Verlag, Berlin.

Hall, I. R., I. N. McCave, M. R. Chapman, and N. J. Shackleton (1998), Coherent deep flow variation in the Iceland and American basins during the last interglacial, *Earth Planet. Sci. Lett.*, *164*, 15–21.

Hall, I. R., I. N. McCave, N. J. Shackleton, G. P. Weedon, and S. E. Harris (2001), Intensified deep Pacific inflow and ventilation in Pleistocene glacial times, *Nature*, *412*, 809–812.

Hays, J. D., J. Imbrie, and N. J. Shackleton (1976), Variations in the Earth's orbit: Pacemaker of the ice ages, *Science*, *194*, 1121–1132.

Henrich, R., K.-H. Baumann, S. Gerhardt, M. Gröger, and A. N. A. Volbers (2003), Carbonate preservation in deep and intermediate water masses in the South Atlantic: Evaluation and geological record (a review), in *The South Atlantic in the Late Quaternary: Reconstructions of Material Budgets and Current Systems*, edited by G. Wefer, S. Mulitza, and V. Ratmeyerl, pp. 645–670, Springer, Berlin.

Hodell, D. A., C. D. Charles, J. H. Curtis, P. G. Mortyn, U. S. Ninnemann, and K. A. Venz (2003), Pleistocene vertical carbon isotope and carbonate gradients in the south Atlantic sector of the Southern Ocean, *Geochem. Geophys. Geosyst.*, *4*(1), 1004, doi:10.1029/2002GC000367.

Howard, W. R., and W. L. Prell (1992), Late Quaternary surface circulation of the southern Indian Ocean and its relationship to orbital variations, *Paleoceanography*, *7*, 79–117.

Imbrie, J., A. McIntyre, and A. Mix (1989), Oceanic response to orbital forcing in the late Quaternary: Observational and experimental strategies, in *Climate and Geosciences: A Challenge for Science and Society in the 21st Century*, edited by A. Berger, J.-C. Duplessy, and S. H. Schneider, pp. 121–164, Reidel, Hingham, Mass.

Johnsen, S. J., et al. (1997), The $\delta^{18}O$ record along the Greenland Ice Core Project deep ice core and the problem of possible Eemian climatic instability, *J. Geophys. Res.*, *102*, 26,397–26,410.

Jouzel, J., et al. (2004), EPICA Dome C ice cores deuterium data, ftp://ftp.ncdc.noaa.gov/pub/data/paleo/icecore/antarctica/epica_domec/edc_dd.txt, Paleoclimatology Program, Natl. Geophys. Data Cent., Boulder, Colo.

Knorr, G., and G. Lohmann (2003), Southern Ocean origin for the resumption of Atlantic thermohaline circulation during deglaciation, *Nature*, *424*, 532–536.

Knutti, R., J. Fluckiger, T. F. Stocker, and A. Timmermann (2004), Strong hemispheric coupling of glacial climate through freshwater discharge and ocean circulation, *Nature*, *430*, 851–856.

Kuhn, G., and B. Diekmann (2002), Late Quaternary variability of ocean circulation in the southeastern South Atlantic inferred from the terrigenous sediment record of a drift deposit in the southern Cape Basin (ODP Site 1089), *Palaeogeogr. Palaeoclimatol. Palaeoecol.*, *182*, 287–303.

Labeyrie, L., et al. (1996), Hydrographic changes of the Southern Ocean (southeast Indian sector) over the last 230 kyr, *Paleoceanography*, *11*, 57–76.

Le, J., and N. J. Shackleton (1992), Carbonate dissolution fluctuations in the western equatorial Pacific during the late Quaternary, *Paleoceanography*, *7*, 21–42.

Lea, D. W. (1995), A trace-metal perspective on the evolution of Antarctic circumpolar deep water chemistry, *Paleoceanography*, *10*, 733–747.

Lutjeharms, J. R. E. (1996), The exchange of water between the South Indian and South Atlantic oceans, in *The South Atlantic: Present and Past Circulation*, edited by G. Wefer et al., pp. 125–162, Springer-Verlag, Berlin.

Lynch-Stieglitz, J., and R. G. Fairbanks (1994), A conservative tracer for glacial ocean circulation from carbon isotope and paleonutrient measurements in benthic foraminifer, *Nature*, *369*, 308–310.

Mackensen, A., and T. Bickert (1999), Stable carbon isotopes in benthic foraminifera: Proxies for deep and bottom water circulation and new production, in *Use of Proxies in Paleoceanography: Examples From the South Atlantic*, edited by G. Fischer and G. Wefer, pp. 229–254, Springer-Verlag, Berlin.

Mackensen, A., H.-W. Hubberten, T. Bickert, G. Fischer, and D. K. Fütterer (1993), The δ^{13}C in benthic for a foraminiferal tests of Fontbotia Wuellerstorfi (Schwager) relative to the δ^{13}C of dissolved inorganic carbon in Southern Ocean deep water: Implications for glacial ocean circulation models, *Paleoceanography*, *8*(5), 587–610.

Mackensen, A., M. Rudolph, and G. Kuhn (2001), Late Pleistocene deep-water circulation in the subantarctic eastern Atlantic, *Global Planet. Change*, *30*, 197–229.

Manighetti, B., and I. N. McCave (1995), Late glacial and Holocene palaeocurrents around Rockall Bank, NE Atlantic Ocean, *Paleoceanography*, *10*, 611–626.

Marchitto, T. M., and W. S. Broecker (2006), Deep water mass geometry in the glacial Atlantic Ocean: A review of constraints from the paleonutrient proxy Cd/Ca, *Geochem. Geophys. Geosyst.*, *7*, Q12003, doi:10.1029/2006GC001323.

Matsumoto, K., and J. Lynch-Stieglitz (1999), Similar glacial and Holocene deep water circulation inferred from southeast Pacific benthic foraminiferal carbon isotope composition, *Paleoceanography*, *14*(2), 149–163.

Matsumoto, K., J. Lynch-Stieglitz, and R. F. Anderson (2001), Similar glacial and Holocene Southern Ocean hydrography, *Paleoceanography*, *16*, 445–454.

McCave, I. N., and I. R. Hall (2006), Size sorting in marine muds: Processes, pitfalls, and prospects for paleoflow-speed proxies, *Geochem. Geophys. Geosyst.*, *7*, Q10N05, doi:10.1029/2006GC001284.

McCave, I. N., B. Manighetti, and N. A. S. Berveridge (1995a), Circulation in the glacial North Atlantic inferred from grain size measurements, *Nature*, *374*, 149–152.

McCave, I. N., B. Manighetti, and S. G. Robinson (1995b), Sortable silt and fine sediment size/composition slicing: Parameters for paleocurrent speed and paleoceanography, *Paleoceanography*, *10*, 593–610.

McCave, I. N., T. Kiefer, D. J. R. Thornalley, and H. Elderfield (2005), Deep flow in the Madagascar-Mascarene Basin over the last 150000 years, *Philos. Trans. R. Soc. London Ser. A*, *363*, 81–99.

McManus, J., G. Bond, W. Broecker, S. J. Johnsen, L. Labeyrie, and S. Higgins (1994), High resolution climate records from the North Atlantic during the last interglacial, *Nature*, *371*, 326–329.

McManus, J. F., R. Francois, J. M. Gherardi, L. D. Kiegwin, and S. Brown-Leger (2004), Collapse and rapid resumption of Atlantic meridional circulation linked to deglacial climate changes, *Nature*, *428*, 834–837.

Michel, E., L. D. Labeyrie, J.-C. Duplessy, N. Gorfti, M. Labracherie, and J.-L. Turon (1995), Could deep subantarctic convection feed the world deep basins during the last glacial maximum?, *Paleoceanography*, *10*, 927–942.

Ninnemann, U. S., and C. D. Charles (2002), Changes in the mode of Southern Ocean circulation over the last glacial cycle revealed by foraminiferal stable isotopic variability, *Earth Planet. Sci. Lett.*, *201*, 383–396.

Nowlin, J. W. D., and J. M. Klinck (1986), The physics of the Antarctic Circumpolar Current, *Rev. Geophys.*, *24*, 469–491.

Oppo, D. W., and R. G. Fairbanks (1987), Variability in the deep and intermediate water circulation of the Atlantic Ocean during the past 25,000 years: Northern Hemisphere modulation of the Southern Ocean, *Earth Planet. Sci. Lett.*, *86*, 1–15.

Oppo, D. W., and M. Horowitz (2000), Glacial deep water geometry: South Atlantic benthic foraminiferal Cd/Ca and $\delta^{13}C$ evidence, *Paleoceanography*, *15*(2), 147–160.

Orsi, A. H., T. Whitworth III, and J. W. D. Nowlin (1995), On the meridional extent and fronts of the Antarctic Circumpolar Current, *Deep Sea Res. Part I*, *42*, 641–673.

Orsi, A. H., G. C. Johnsen, and J. L. Bullister (1999), Circulation mixing and production of Antarctic bottom water, *Prog. Oceanogr.*, *43*, 55–109.

Pahnke, K., and R. Zahn (2005), Southern Hemisphere water mass conversion linked with North Atlantic climate variability, *Science*, *307*, 1741–1746.

Pahnke, K., R. Zahn, H. Elderfield, and M. Schulz (2003), 340,000 year centennial-scale marine record of Southern Hemisphere climate oscillation, *Science*, *301*, 948–952.

Peeters, F. J. C., R. Acheson, G.-J. A. Brummer, W. P. M. De Ruijter, R. R. Schneider, G. M. Ganssen, E. Ufkes, and D. Kroon (2004), Vigorous exchange between the Indian and Atlantic oceans at the end of the past five glacial cycles, *Nature*, *430*, 661–665.

Petit, J. R., et al. (1999), Climate and atmospheric history of the past 420,000 years from the Vostok ice core, Antarctica, *Nature*, *399*, 429–436.

Pfuhl, H. A., and N. J. Shackleton (2004), Two proximal, high resolution records of foraminiferal fragmentation and their implications for changes in dissolution, *Deep Sea Res. Part I*, *51*, 809–832.

Piotrowski, A. M., S. L. Goldstein, S. R. Hemming, and R. G. Fairbanks (2004), Intensification and variability of ocean thermohaline circulation through the last deglaciation, *Earth Planet. Sci. Lett.*, *225*, 205–220.

Piotrowski, A. M., S. L. Goldstein, S. R. Hemming, and R. G. Fairbanks (2005), Temporal relationships of carbon cycling and ocean circulation at glacial boundaries, *Science*, *307*, 1933–1938.

Pudsey, C. J., and J. A. Howe (1998), Quaternary history of the Antarctic Circumpolar Current: Evidence from the Scotia Sea, *Mar. Geol.*, *148*, 83–112.

Reid, J. L. (1989), On the total geostrophic circulation of the South Atlantic Ocean: Flow patterns, tracers, and transports, *Prog. Oceanogr.*, *23*, 149–244.

Reid, J. L. (2005), On the world-wide circulation of the deep water from the North Atlantic Ocean, *J. Mar. Res.*, *63*, 187–201.

Richardson, P. L., J. R. E. Lutjeharms, and O. Boebel (2003), Introduction to the ''Inter-ocean exchange around southern Africa,'' *Deep Sea Res. Part II*, *50*, 1–12.

Rosenthal, Y., E. A. Boyle, and L. Labeyrie (1997), Last Glacial Maximum paleochemistry and deepwater circulation in the Southern Ocean: Evidence from foraminiferal cadmium, *Paleoceanography*, *12*(6), 787–796.

Rutberg, R. L., S. R. Hemming, and S. L. Goldstein (2000), Reduced North Atlantic deep water flux to the glacial Southern Ocean inferred from neodymium isotope ratios, *Nature*, *405*, 935–938.

Sarnthein, M., and R. Tiedemann (1990), Younger Dryas-style cooling events at glacial terminations I-VI: Associated benthic delta13C anomalies ad ODP site 658 constrain meltwater hypothesis, *Paleoceanography*, *5*, 1041–1055.

Sarnthein, M., K. Winn, S. J. A. Jung, J.-C. Duplessy, L. Labeyrie, H. Erlenkeuser, and G. Ganssen (1994), Changes in east Atlantic deepwater circulation over the last 30000 years: Eight time slice reconstructions, *Paleoceanography*, *9*, 209–268.

Schlitzer, R. (2000), Electronic atlas of WOCE hydrographic and tracer data, *Eos Trans. AGU*, *81*(5), 45.

Schrag, D. P., J. F. Adkins, K. McIntyre, J. L. Alexander, D. A. Hodell, C. D. Charles, and J. F. McManus (2002), The oxygen isotopic composition of seawater during the Last Glacial Maximum, *Quat. Sci. Rev.*, *21*, 331–342.

Seidov, D., B. J. Haupt, E. J. Barron, and M. Maslin (2001), Ocean bi-polar seesaw and climate: Southern versus northern meltwater impacts, in *The Ocean and Rapid Climate Change: Past, Present and Future*, *Geophys. Monogr. Ser.*, vol. 126, edited by D. Seidov, B. J. Haput, and M. Maslin, pp. 147–167, AGU, Washington, D. C.

Shackleton, N. J., and M. A. Hall (1997), The late Miocene stable isotope record, site 926, *Proc. Ocean Drill. Program Sci. Results*, *154*, 367–373.

Shackleton, N. J., M. A. Hall, and E. Vincent (2000), Phase relationships between millennial-scale events 64,000-24,000 years ago, *Paleoceanography*, *15*(6), 565–569.

Siddall, M., E. Bard, E. J. Rohling, and C. Hemleben (2006), Sea-level reversal during termination II, *Geology*, *34*, 817–820.

Sigman, D. M., and E. A. Boyle (2000), Glacial/interglacial variations in atmospheric carbon dioxide, *Nature*, *407*, 859–869.

Sikes, E. L., C. R. Samson, T. P. Guilderson, and W. R. Howard (2000), Old radiocarbon ages in the southwest Pacific Ocean during the last glacial period and deglaciation, *Nature*, *405*, 555–559.

Sloyan, B. M., and R. S. Rintoul (2001), Circulation, modification, and renewal of Antarctic mode and intermediate water, *J. Phys.*, 31,1005–31,1030.

Spero, H. J., and D. W. Lea (2002), The cause of carbon isotope minimum events on glacial terminations, *Science*, *296*, 522–525.

Stocker, T. F., and S. J. Johnsen (2003), A minimum thermodynamic model for the bipolar seesaw, *Paleoceanography*, *18*(4), 1087, doi:10.1029/2003PA000920.

Streeter, S. S., and N. J. Shackleton (1979), Paleocirculation of the deep North Atlantic: 150,000-year record of benthic foraminifera and oxygen-18, *Science*, *203*, 168–171.

Tucholke, B. E., and G. B. Carpenter (1977), Sediment distribution and Cenozoic sedimentation patterns on Agulhas Plateau, *Geol. Soc. Am. Bull.*, *88*, 1337–1346.

Uenzelmann-Neben, G. (2001), Seismic characteristics of sediment drifts: An example from the Agulhas Plateau, southwest Indian Ocean, *Mar. Geophys. Res.*, *22*, 323–343.

Uenzelmann-Neben, G. (2002), Contourites on the Agulhas Plateau, SW Indian Ocean: Indications for the evolutions of currents since Paleogene times, in *Deep-water Contourite Systems: Modern Drifts and Ancient Series, Seismic and Sedimentary Characteristics*,

Geol. Soc. Mem., vol. 22, edited by D. Stow et al., pp. 271–288, Geol. Soc. of London, London.

Volbers, A. N. A., and R. Henrich (2004), Calcium carbonate corrosiveness in the South Atlantic during the Last Glacial Maximum as inferred from changes in the preservation of Globigerina bulloides: A proxy to determine deep-water circulation patterns?, *Mar. Geol.*, *204*, 43–57.

Waelbroeck, C., L. Labeyrie, E. Michel, J.-C. Duplessy, J. McManus, K. Lambeck, E. Balbon, and M. Labracherie (2002), Sea-level and deep water temperature changes derived from benthic foraminifera isotopic records, *Quat. Sci. Rev.*, *21*, 295–305.

Weaver, A. J., O. A. Saenko, P. U. Clark, and J. X. Mitrovica (2003), Meltwater pulse 1A from Antarctica as a trigger of the Bolling-Allerod warm interval, *Science*, *299*, 1709–1713.

Weijer, W., W. P. M. de Ruijter, A. Sterl, and S. S. Drijfhout (2002), Response of the Atlantic overturning circulation to South Atlantic sources of buoyancy, *Global Planet. Change*, *34*, 293–311.

Whitworth, T., III, and R. G. Peterson (1985), Volume transport of the Antarctic Circumpolar Current from bottom pressure measurements, *J. Phys. Oceanogr.*, *15*, 810–816.

Yu, E.-F., R. Francois, and M. P. Bacon (1996), Similar rates of modern and last glacial ocean thermohaline circulation inferred from radiochemical data, *Nature*, *379*, 689–694.

P. Diz, I. R. Hall, and E. G. Molyneux, School of Earth, Ocean, and Planetary Sciences, Cardiff University, Main Building, Park Place, Cardiff CF10 3YE, UK. (molyneuxeg@cardiff.ac.uk)

R. Zahn, Institució Catalana de Recerca i Estudis Avançats, Institut de Ciencia i Tecnología Ambientals, Universitat Autónoma de Barcelona, Edificio Ciències, E-08193 Bellaterra, Spain.